Supplementary materials:

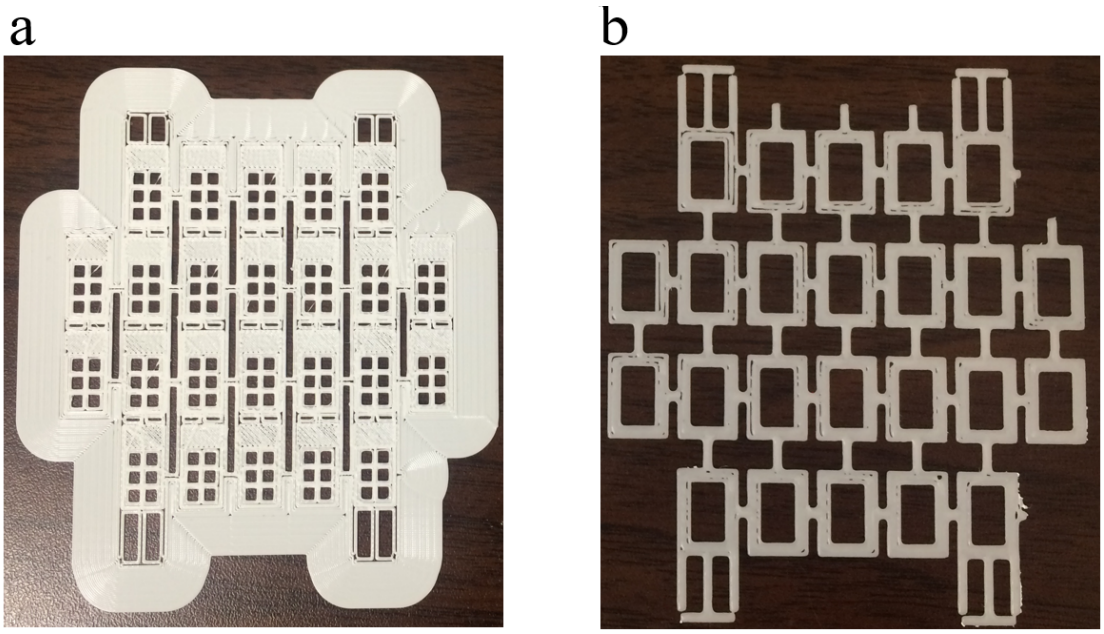

Figure S1. (**a**) 3D-printed wafer-scale PLA holder. (**b**) 3D-printed wafer-scale Emate material with low melting temperature.

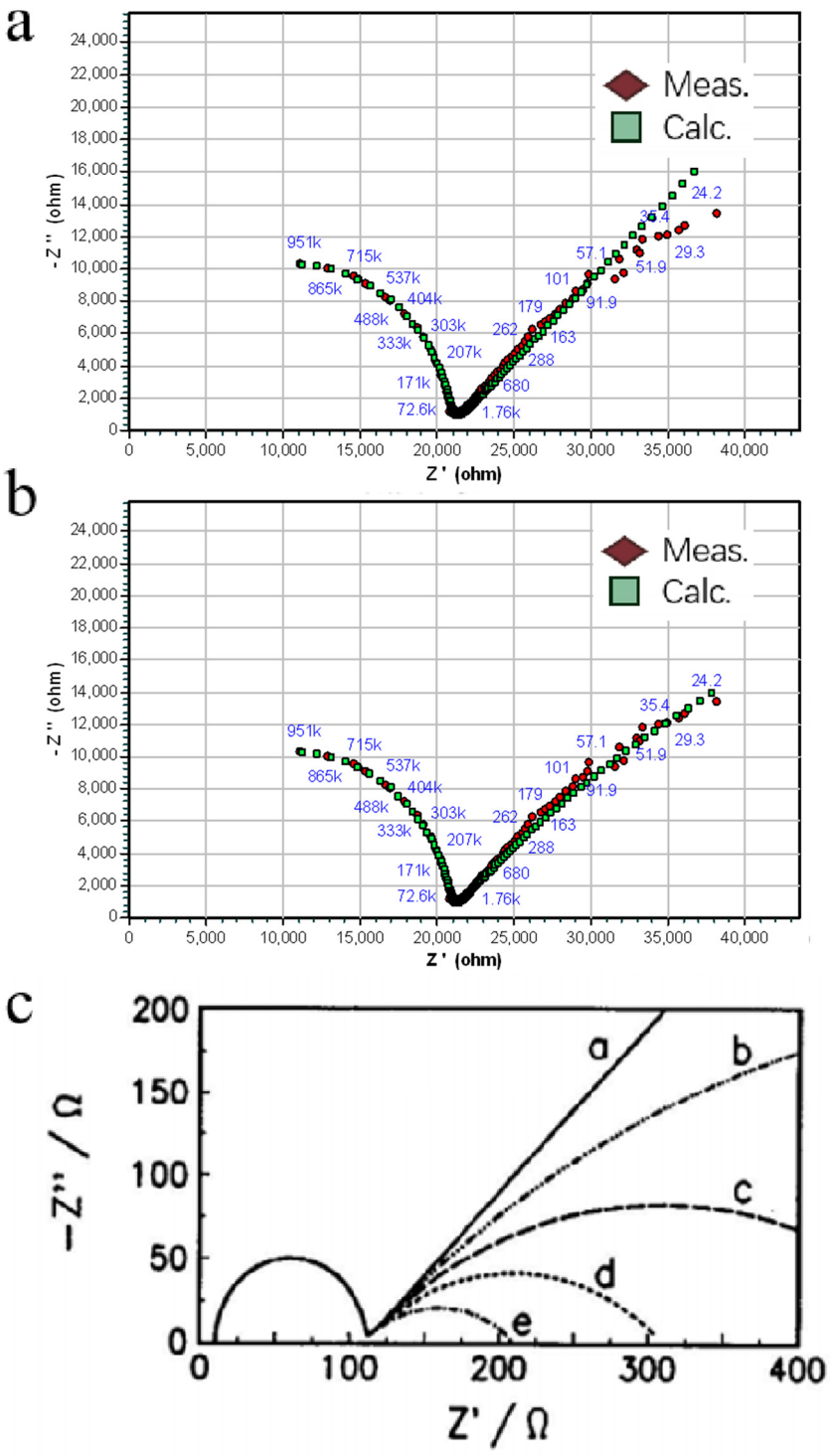

Figure S2. (**a**) Measurement data (red) and fitted data (green) with Randles model of the DI water impedance measurement on the NC membrane. (**b**) This figure shows the measurement data in (a) fitted with the "improved model" for low concentrations. (**c**) Nyquist plot of electrodes of different radii, where curve a is a planar electrode and e is a circular electrode with the smallest radius [1].

Analysis of Figure S2

The Nyquist plot of the bacterial impedance measurement is shown in red points in Figure S2a, while the fitting data based on the Randles model is plotted with green dots. It is observed that the

low-frequency region significantly differs between the measurement and fitting data. At low frequencies, the process of sensing bacteria is mass-transfer-controlled, while at high frequencies, bacterial sensing is controlled by kinetics [35]. The mass-transfer-controlled region in Figure S2a approximates a linear part, representing the diffusion-limited process. In the kinetics-controlled region, the diameter of the semicircle on the Nyquist plot indicates electron transfer resistance, R_{ct}, according to the literature [35–37].

As shown in Figure 2c, we observed that electrodes on the filter membrane are similar to a network of tiny, connected wires. Those wires had curved interfaces with the solution. This feature makes the surface of our IDT electrode unable to be considered as an ideal planar capacitance. Due to this, we used the constant phase element (CPE), Q, to replace the capacitance, C, in our model. CPE is an electrical component commonly used in electrochemistry. Similar to a capacitor, but with a non-linear phase response in frequency, CPE is typically used to describe systems with non-ideal electrochemical interfaces, such as those with surface roughness, porosity, or unevenly distributed reactants. We improved two places in the Randles model with CPE: (1) we used CPE to replace the ideal double-layer capacitor, and (2) we replaced the Warburg impedance with a QR loop because the Warburg impedance models a planar electrode's diffusion process. By incorporating CPE into the Randles model, we enhanced its alignment with the actual conditions of our paper-based sensors, resulting in a more accurate fitting of the curve.

According to "Semiconductors and Mott-Schottky Plots" [39], the impedance in a Nyquist plot is closer to an ellipse shape as the radius of circular electrodes becomes smaller (Figure S2c). This means if the surface of the electrode became more irregular or less like an ideal surface, the low-frequency region would be characterized by a greater deviation from curve a (Figure S2c), which represents the ideal planar capacitance.

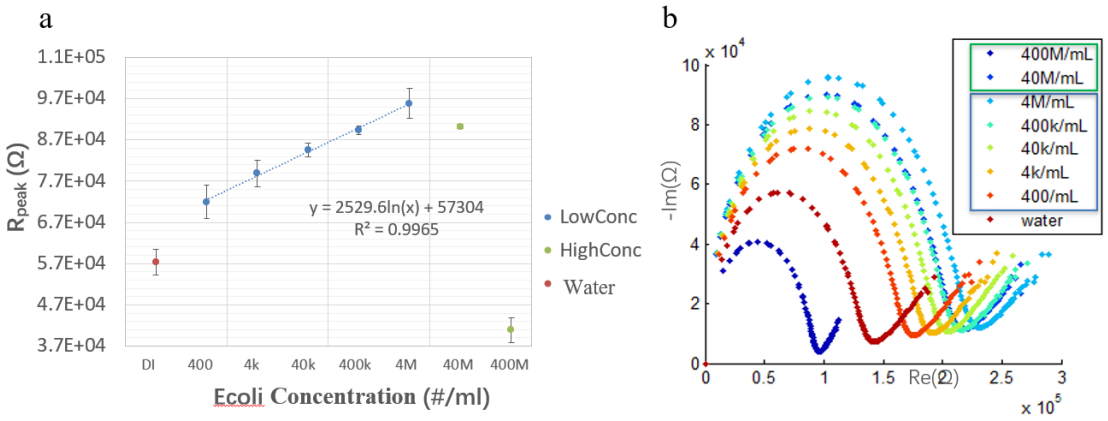

Figure S3. (**a**) The peak of the semicircle part of the impedance measurement of DI water, 40–400 M cells per milliliter. (**b**) The Nyquist plot of DI water, 40–400 M cells per milliliter.

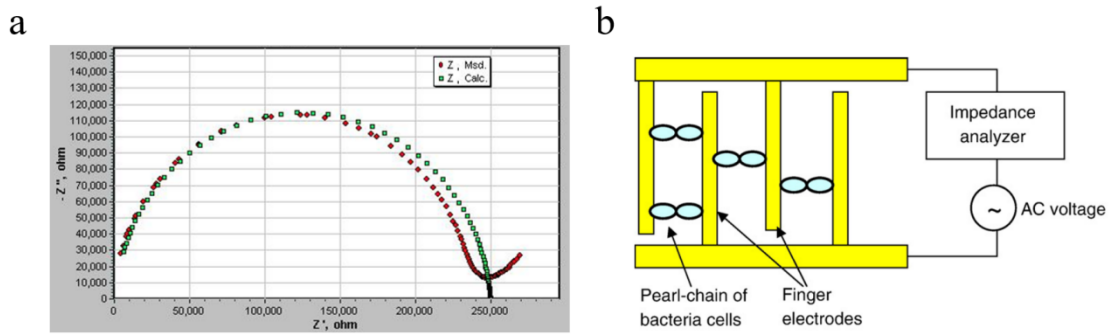

Figure S4. (**a**) Fitting (green) the measured data (red) of 40 M/mL (red) with the improved model for low concentrations. (**b**) The pearl chain effect of bacteria cells between the two IDT electrodes.

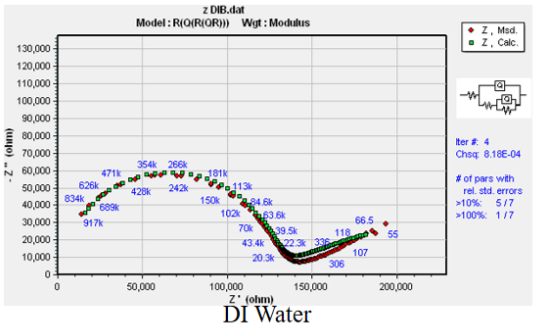

DI Water

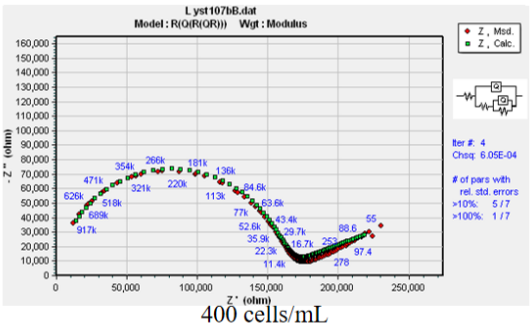

400 cells/mL

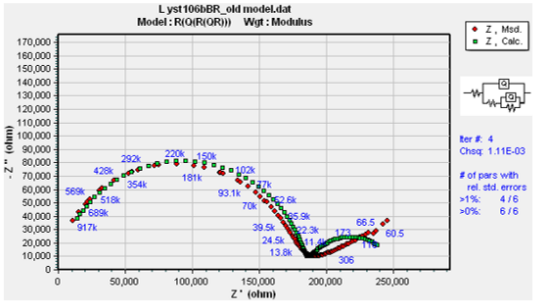

4k cells/mL

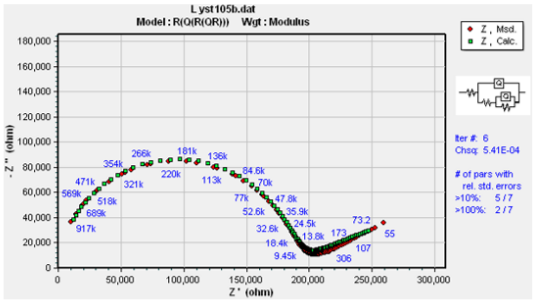

40k cells/mL

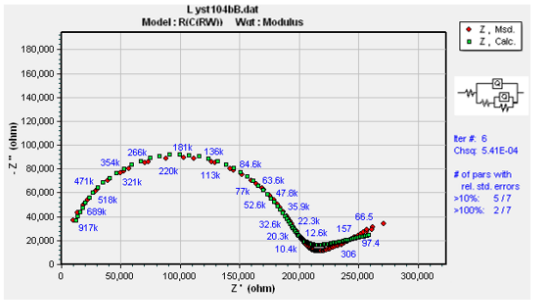

400k cells/mL

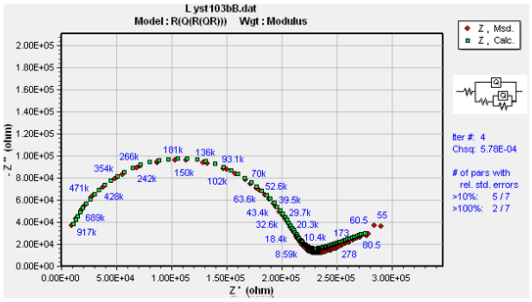

4M cells/mL

Fit by Improved Model

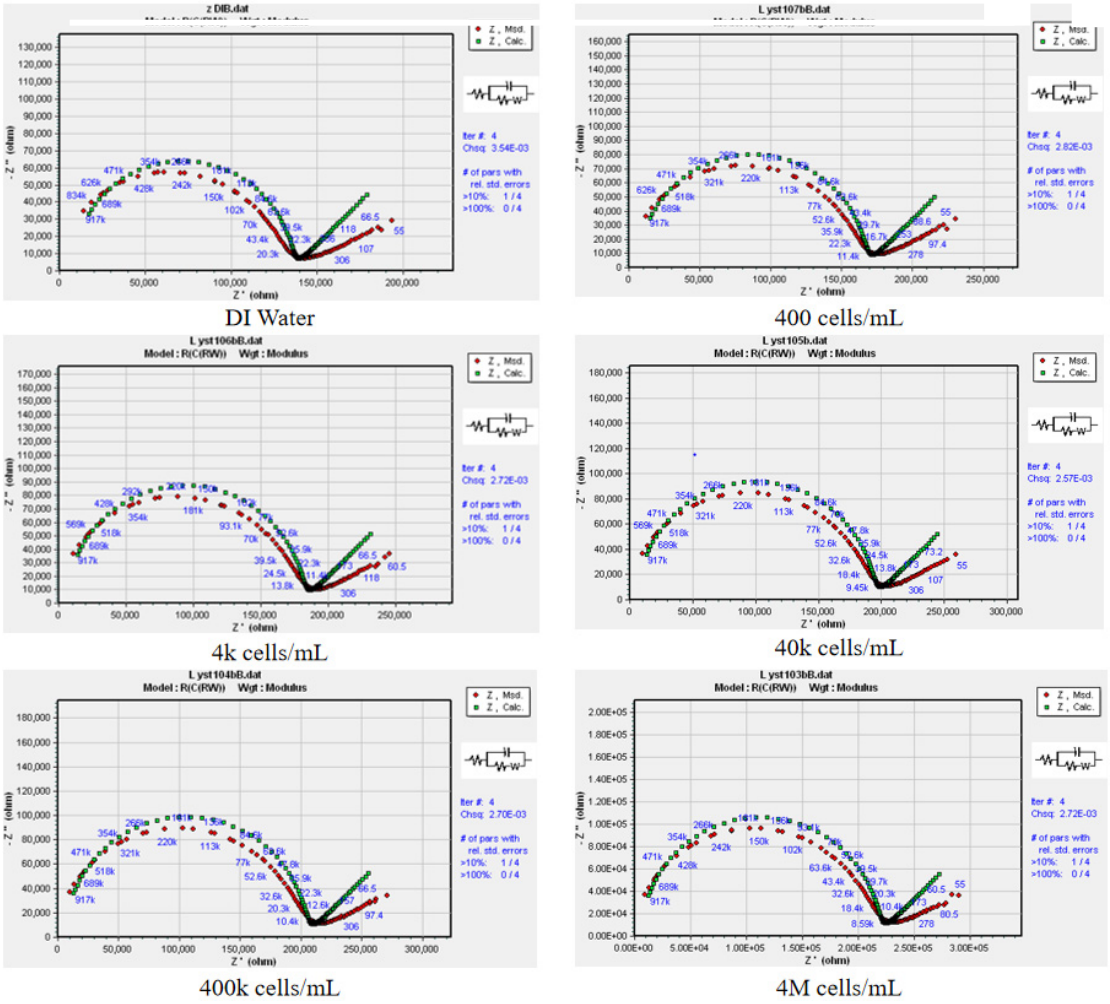

Fit by Randles Model

Figure S5. Fitting (green) the measured data (red) of DI water, 400, 4,000, 40,000, 400,000, and 4M, cells/mL, with the improved model for low concentrations and the Randles model.

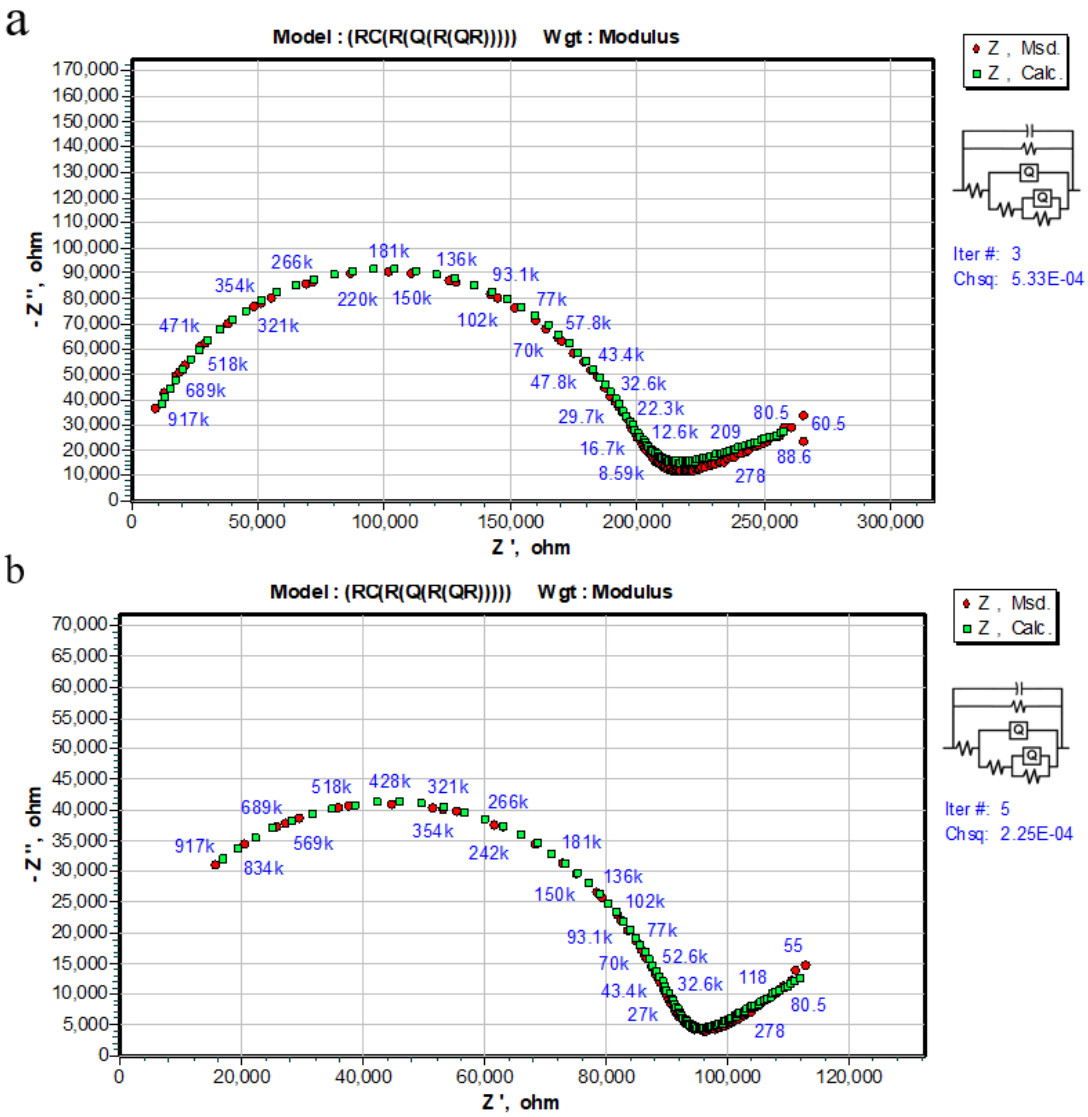

Figure S6. Fitting (green) the measured data (red) of (**a**) 40 M and (**b**) 400 M cells/mL (red) with the high-concentration model.

Figure S7. (left) The demonstration of the actual image of the sensor during testing, and (right) the comparison of the sensor layer and a US quarter dollar.

We conducted more experiments to prove our pearl effect theory. Below, Figure S8a,b show the testing data and the zoom-in plot of *E. Coli* in urine. We observed that when the concentration increased, the impedance response curve started at the simulated urine (orange line, which contains no bacteria), then shifted to the right (R_{ct} increased) first, then to the left (R_{ct} decreased). The general trend is the same as the sample of water.

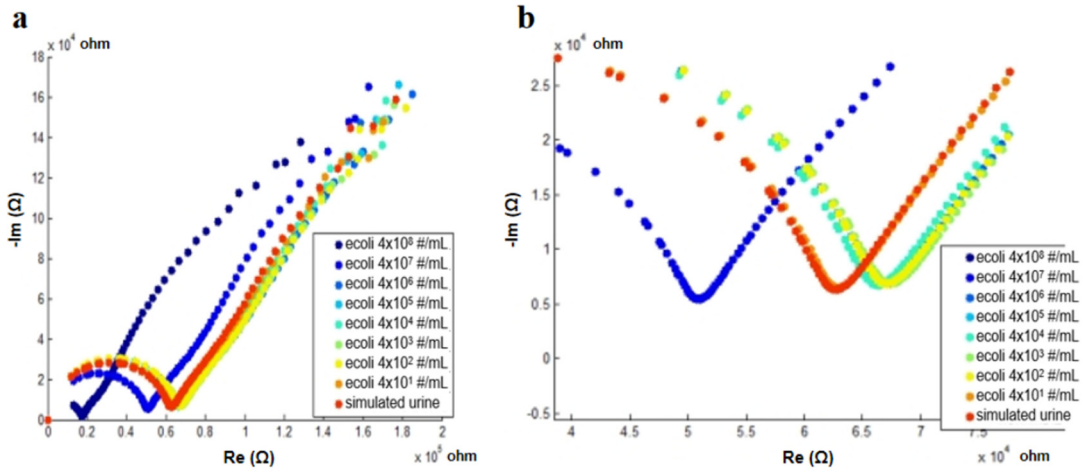

Figure S8. (**a**) The Nyquist plot of measurement data for *E. coli* in urine. (**b**) The zoom-in image of the experiment data in Figure S8a.

Additionally, we tested our sensor's performance with another bacteria sample. Figure S9 shows the result when using yeast as the detection target.

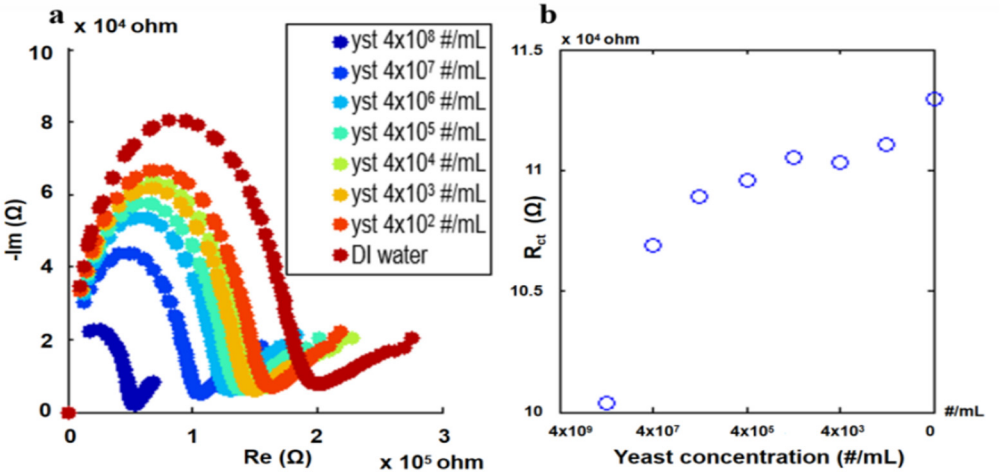

Figure S9. (**a**) Nyquist plot of measurement data for yeast samples. (**b**) Extracted charge transfer resistance (R_{ct}) decreased as the yeast concentration increased.

When using yeast as the target, the response curve of impedance was similar to the result using *E. coli* (the left picture). However, the size of the yeast was much larger than *E. coli*. We observed that the R_{ct} immediately decreased when the concentration increased. We considered that the pearl chain effect occurred immediately when the yeast concentration exceeded 4×10^2 cells/mL, which caused this phenomenon. The linear relationship between R_{ct} and the yeast concentration was not as good as that for *E. coli* (the right picture).